Some evidence of aviation fingerprint in diurnal cycle of cirrus over the North Atlantic

K. Graf*, H. Mannstein, B. Mayer, U. Schumann
Deutsches Zentrum für Luft- und Raumfahrt, Institut für Physik der Atmosphäre, Oberpfaffenhofen, Germany

Keywords: Contrail, Contrail Cirrus, Aviation

ABSTRACT: The diurnal cycle of aviation in the North Atlantic Region (NAR; 45° W – 10° W, 45° N – 55° N) shows a unique fingerprint dominated by two maxima due to rush-hours in westbound resp. eastbound air traffic. We investigate the hypothesis that this signature can be found also in the diurnal cycle of cirrus coverage. Air traffic data were kindly provided by EUROCONTROL with adequate temporal and spatial resolution for this investigation. The cirrus cover is derived from Meteosat-8/9 SEVIRI data with a spatial resolution of about 5 km and a temporal resolution of 15 min using the cirrus detection algorithm MeCiDA (Krebs et al., 2007). Aviation induced cloud cover changes are derived from diurnal cycle of cirrus cover observed in NAR. We developed several response functions representing the effect of air traffic on cirrus coverage and applied fitting methods for determination of the fit parameters representing the statistical lifetime and the amount of AIC in NAR. Application of the fitting procedures to the air traffic density (ATD) allows us to reproduce the signature of cirrus coverage observed in cirrus coverage. The results are robust for investigations of sub regions of NAR with different signatures of initial ATD and shifts in the occurrence of maxima. Several satellite scenes illustrate the statistical behaviour in single scenes.

1 DATASETS – CIRRUS COVERAGE AND AIR TRAFFIC DENSITY

The MSG cirrus detection algorithm MeCiDA (Krebs et al., 2007) using seven infrared channels of MSG-SEVIRI is applied, delivering a time series of cirrus coverage for the considered region with a temporal resolution of 15 minutes.

* *Corresponding author:* Kaspar Graf, Deutsches Zentrum für Luft- und Raumfahrt, Institut für Physik der Atmosphäre, Oberpfaffenhofen, Germany. Email: Kaspar.Graf@dlr.de

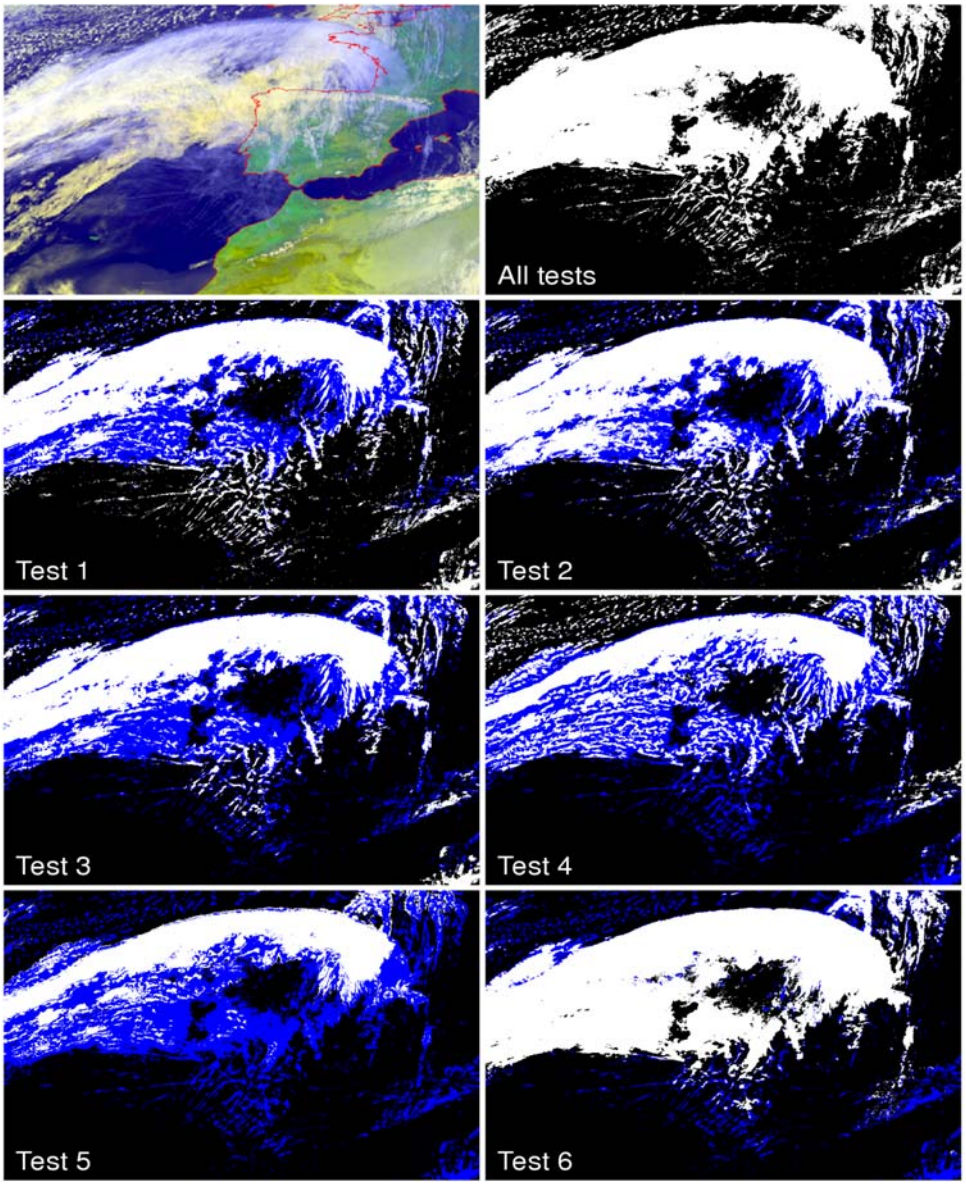

Figure 1. Top left: False color composit of an exemplary cirrus scene. Top right: MeCiDA cirrus classification. The resulting cirrus classification is a combination of six individual cirrus tests which are combined by a logical "OR", see Krebs et al. (2007).

Based on this time series the diurnal cycle of cirrus coverage in NAR can be obtained. Missing time steps (e.g. satellite malfunction) are interpolated. The diurnal cycle for several sub regions of NAR is determined similarly. The algorithm was applied to a four year time period (02/2004 –01/2008). Within the ESA-DUE Project CONTRAILS, EUROCONTROL provided a dataset of air traffic density (ATD) for six weeks in 2004 with a temporal resolution of 15 min and a spatial resolution of 0.25° x 0.25° for the region shown in figure 2.

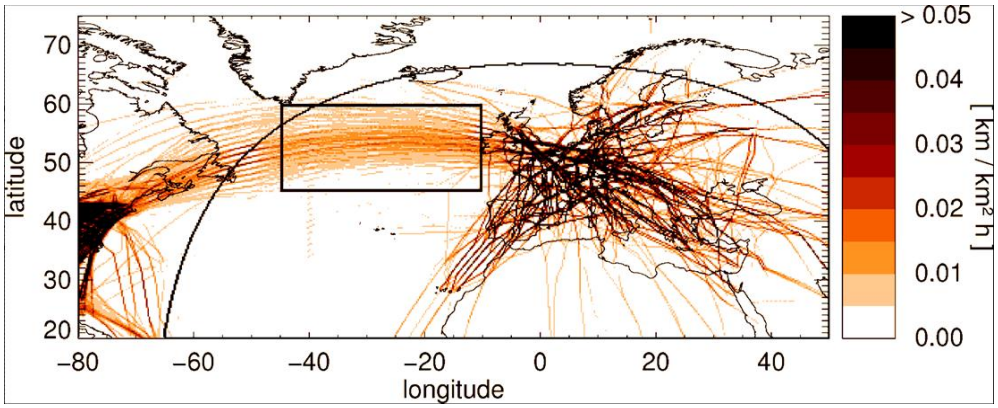

Figure 2. Mean air traffic density in Europe and the North Atlantic. The region NAR is marked by the box. The curve is representing the 75° satellite zenith angle of Meteosat-8/9.

This dataset allows the determination of a representative diurnal cycle of ATD in the NAR, showing a peak at 4 am (UTC) representing the eastbound transatlantic rush hour whereas the peak at 4 pm represents the maximum in westbound traffic.

2 METHOD

The mean diurnal cycle of cirrus coverage shows a pattern similar to a delayed ATD diurnal cycle.

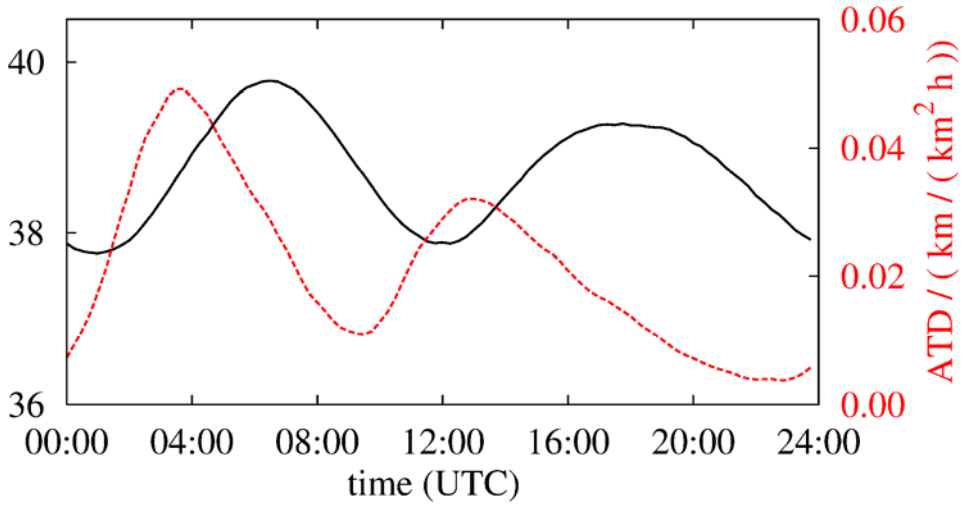

Figure 3. Mean diurnal cycle of air traffic density in NAR (red) and observed cirrus coverage in the same region (black) for 2004.

The diurnal cycle of cirrus coverage can be described as a composite of a constant background, a natural diurnal cycle and an AIC component:

$$C(t) = C_{mean} + C_0(t) + c_{AIC}(t)$$

The natural diurnal cycle $C_0(t)$ is either assumed to be negligible or assumed to be identical to the one observed in the corresponding South Atlantic Region SAR. The AIC contribution to the cirrus cover at time t, $c_{AIC}(t)$ can be expressed statistically as a superposition of all air traffic events in the past,

$$c_{AIC}(t) = \int_{-\infty}^{t} a(t') \cdot r(t-t')\, dt',$$

where r is representing the mean AIC at time t triggered by an air traffic event at time t'. For quantification of AIC, we use several response functions r(t) representing this answer of cirrus cover to an air traffic event:

$$r_1(t) = s \cdot \delta(t-\tau), \quad \delta(t) = 0 \ for\ t \neq 0, \quad \int_{-\infty}^{\infty} \delta(t)\, dt \equiv 1$$

$$r_2(t) = \begin{cases} s \cdot t \cdot e^{-\lambda \cdot t} & for\ t \geq 0 \\ 0 & for\ t < 0 \end{cases}$$

$$r_3(t) = b \cdot t^c \cdot e^{-d \cdot t} \cdot e^{-f \cdot t^2}$$

$$r_4(t) = b \cdot t^c \cdot e^{-d \cdot (t-f)^g}$$

Based on the ATD, the coefficients of the response functions are least-square-fitted to the cycle in cirrus coverage (see Fig. 4)

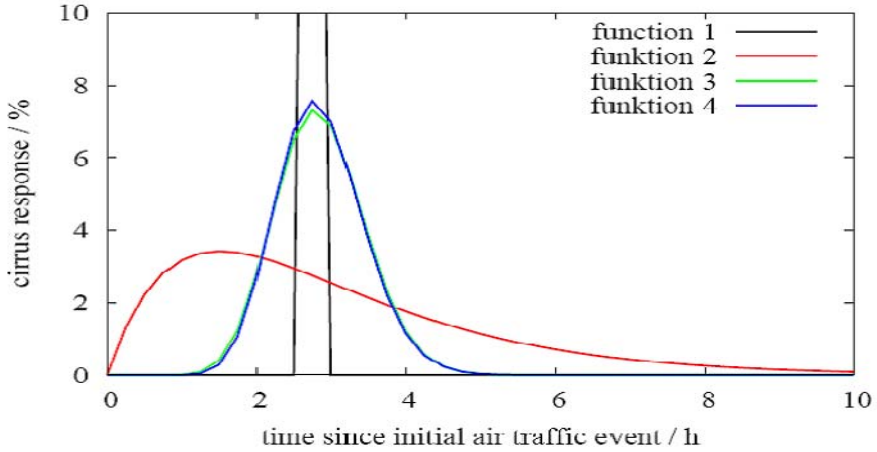

Figure 4. Shape of the different response functions declared in the text.

3 RESULTS

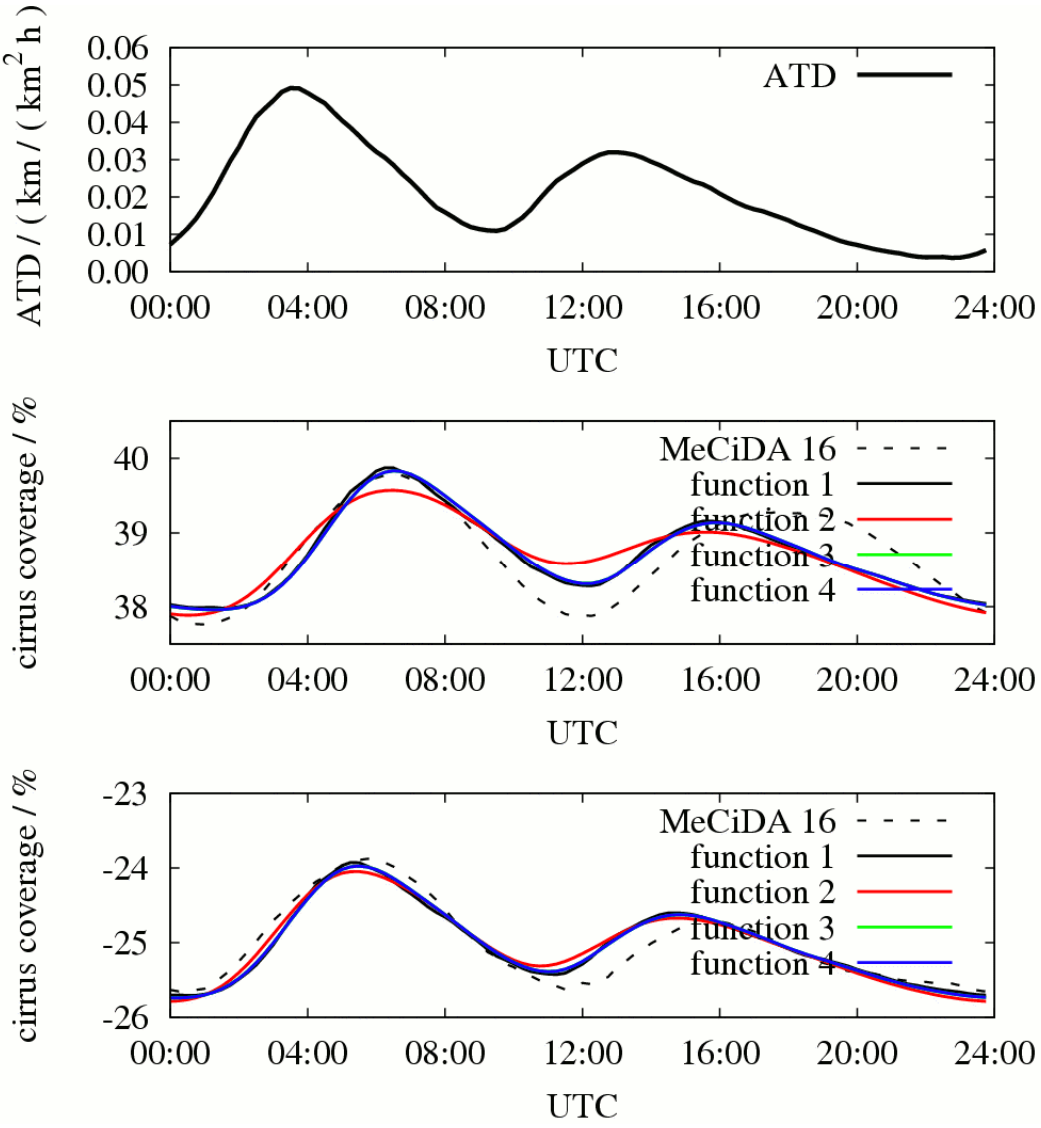

Figure 5. Diurnal cycle of ATD in NAR, based on six weeks in 2004 (top), observed and fitted diurnal cycle of cirrus coverage for the cases $C_0(t) = 0$ (middle) and $C_0(t) = C_{SAR}(t)$ (bottom).

On figure 5, the fitting results based on the ATD input (top) are shown for the case $C_0(t) = 0$ (middle) and $C_0(t)=C_{SAR}(t)$ (bottom). It is obvious that the fitting result is different for each response function. In general, the fitting procedure performs better for the case $C_0(t) = C_{SAR}(t)$.

Table1. Fitting results for response functions r_1, r_2, r_3 and r_4 as declared in the text.

nr	$C_0(t)$	C_{Mean}	s	τ in h	-	-	-	ρ	Δc	c_{AIC}
1	0	0.378	0.416	2.75	-	-	-	0.871	0.003	0.0083
1	SAR	-0.259	0.392	1.75	-	-	-	0.946	0.017	0.0083
			s	λ	-	-	-			
2	0	0.375	0.061	0.66	-	-	-	0.790	0.0038	0.0119
2	SAR	-0.26	0.145	1.11	-	-	-	0.940	0.0019	0.0098
			b	c	d	f	-			
3	0	0.378	0.0044	7.05	0.345	0.71	-	0.867	0.0031	0.0095
3	SAR	-0.259	0.0864	2.89	0.428	0.39	-	0.949	0.0017	0.0089
			b	c	d	f	g			
4	0	0.378	0.5605	17.39	1.50	2.25	1.60	0.870	0.0031	0.0092
4	SAR	-0.259	3.7676	4.51	1.10	1.61	1.48	0.949	0.0017	0.0089

The fit parameters are shown in table 1. For fit function 1 (simple delay), best fits are obtained for a time shift of 1.75 resp. 2.75 h. The 24-h mean AIC in NAR is 0.83% in both cases. For the other response functions, AIC amounts to about 0.8 – 1.2%, depending on which assumption for $C_0(t)$ is used. All results shown here are based on data from February – December 2004, as for the following years no representative ATD dataset is available so far.

4 CONSISTENCY

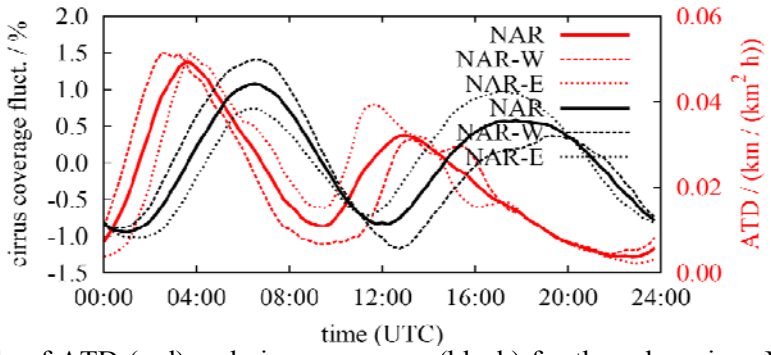

Figure 6. Diurnal cycle of ATD (red) and cirrus coverage (black) for the sub regions NAR-W and NAR-E, the western resp. eastern part of NAR.

The peak representing ATD in eastbound direction occurs earlier in the western part of NAR than in the eastern one, whereas the westbound peak occurs earlier in the eastern part of the NAR. This unique (i.e. non-meteorological) behaviour can be retrieved in the cirrus coverage as well (Fig. 6).

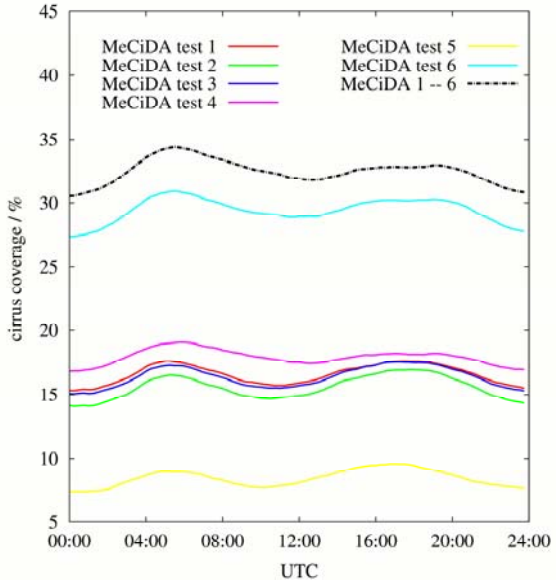

Figure 7. Diurnal cycle of cirrus coverage derived by the six individual cirrus tests of MeCiDA for NAR, 2004.

MeCiDA consists of six individual cirrus tests based on different channel combinations of MSG-SEVIRI. These tests are combined by a logical "OR". Applying each test alone to a data-subset, the diurnal cycle in cirrus coverage is consistent with the total MeCiDA result (see figure 7). Therefore, artefacts due to a "diurnal-cycle sensitive" channel (e.g. the ozone channel 9.3 μm) are excluded. Furthermore, periodic oscillations of MSG around its nominal position were analysed. The frequency of these oscillations would not cause a diurnal cycle.

5 EXAMPLE AND OUTLOOK

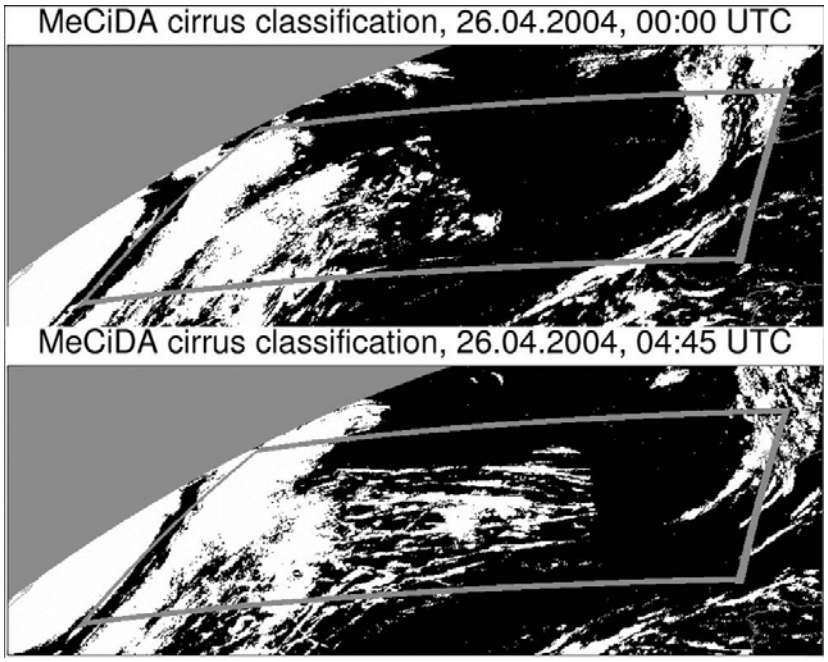

Figure 8. Cirrus scenes derived with MeCiDA.

The visibility of AIC in satellite data is illustrated by the two scenes shown in figure 8: At 0:00 UTC, ATD is low and the last peak was 10 hours ago. Therefore, no significant ATD fingerprints are visible in the satellite scene. At 4:45 UTC, the westbound ATD has passed the region two hours ago and triggered AIC in the NAR. In the following time, this AIC is decreasing until the eastbound ATD triggers new AIC formation. Further work is needed for a better identification and understanding of natural contributions in diurnal cycle of cirrus coverage in NAR as well as SAR.

The HALO campaign "ML-CIRRUS" will address the validation of diurnal cycle in AIC. So far, analysis is based on an ATD dataset of several weeks. A complete ATD dataset is needed for a more detailed consistency check and for comparisons with the Contrail and Cirrus Prediction tool CoCiP (Schumann, 2009).

6 ACKNOWLEDGEMENT

We thank S. Rentsch for data handling support. Meteosat 8/9 data were provided by EUMETSAT via the German Sensing data center at DLR and air traffic data were provided by EUROCONTROL, both within the ESA-DUE project CONTRAILS. The work performed was part of the DLR projects PAZI 2 and CATS, and the BMBF project UFO within Klimazwei.

REFERENCES

Krebs, W., H. Mannstein, L. Bugliaro, and B. Mayer, 2007, Technical note: A new day- and night-time Meteosat Second Generation Cirrus Detection Algorithm MeCiDA. Atmos. Chem. Phys., 7, 6145-6159

Schumann, U., 2009: A Contrail Cirrus Prediction Tool. In: Sausen, R. et al. (eds.): Proceedings of an International Conference on Transport, Atmosphere and Climate (TAC-2). Aachen, Maastricht, 2009, in press